JAAS

Accepted Manuscript

This is an *Accepted Manuscript*, which has been through the Royal Society of Chemistry peer review process and has been accepted for publication.

Accepted Manuscripts are published online shortly after acceptance, before technical editing, formatting and proof reading. Using this free service, authors can make their results available to the community, in citable form, before we publish the edited article. We will replace this *Accepted Manuscript* with the edited and formatted *Advance Article* as soon as it is available.

You can find more information about *Accepted Manuscripts* in the Information for Authors.

Please note that technical editing may introduce minor changes to the text and/or graphics, which may alter content. The journal's standard Terms & Conditions and the Ethical guidelines still apply. In no event shall the Royal Society of Chemistry be held responsible for any errors or omissions in this *Accepted Manuscript* or any consequences arising from the use of any information it contains.

ROYAL SOCIETY OF CHEMISTRY

www.rsc.org/jaas

This article demonstrates the potential of HR CS GFMAS for providing Br isotopic information, and the benefits of ID for solid sampling.

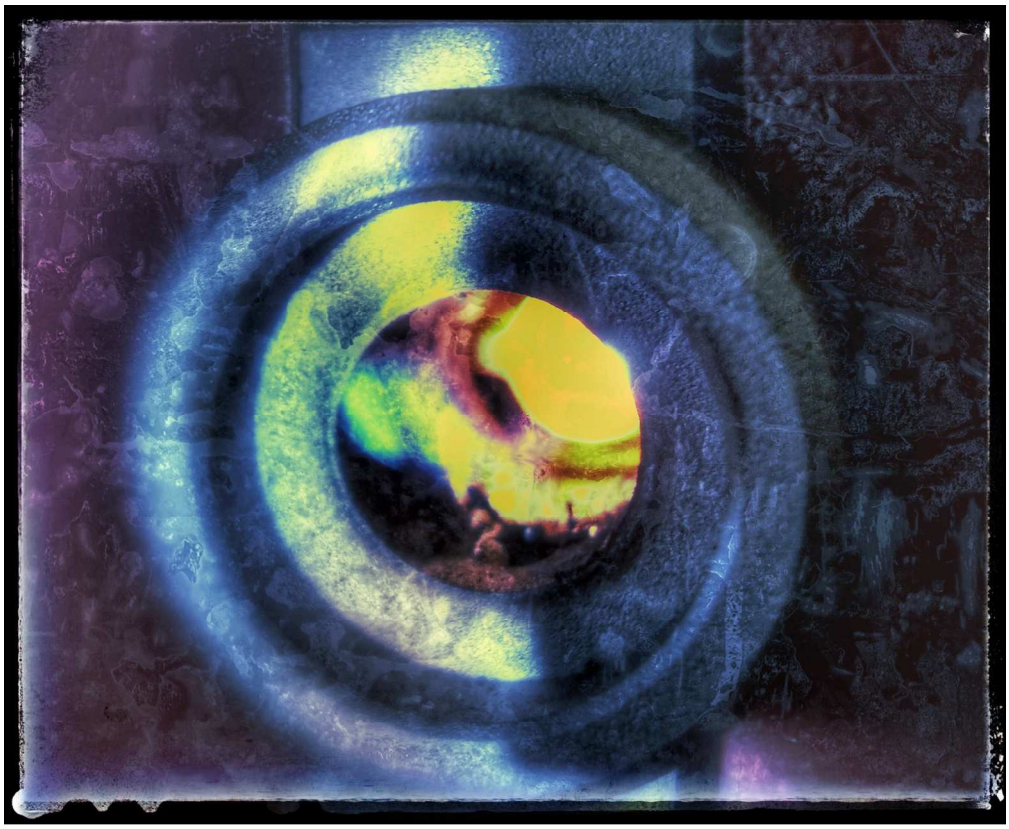

562x460mm (72 x 72 DPI)

Br isotope determination *via* the monitoring of CaBr transitions using high-resolution continuum source graphite furnace molecular absorption spectrometry. Potential for direct determination of Br in solid samples using isotope dilution.

F. V. Nakadi,[ab] M. A. M. S. da Veiga,[ab] M. Aramendía,[ac] E. García-Ruiz[a] and M. Resano*[a]

[a]Department of Analytical Chemistry, Aragón Institute of Engineering Research (I3A), University of Zaragoza, Pedro Cerbuna 12, 50009, Zaragoza, Spain. E-mail: mresano@unizar.es

[b]While on leave from Departamento de Química, Faculdade de Filosofia, Ciências e Letras de Ribeirão Preto, Universidade de São Paulo, 14040-901, Ribeirão Preto-SP, Brazil

[c]Centro Universitario de la Defensa-Academia General Militar de Zaragoza, Carretera de Huesca s/n, 50090, Zaragoza, Spain

Abstract

This work investigates the possibility of obtaining Br isotopic information by generating a gaseous diatomic molecule in a graphite furnace and monitoring its absorption spectrum using a high-resolution continuum source device (HR CS GFMAS). Different metals (Al, Ba, Ca) were investigated to produce this diatomic molecule and the most promising results, both in terms of isotopic shift and sensitivity, were obtained with Ca, thus leaving CaBr as the target species.

The results demonstrate that, unlike what occurs when monitoring atomic spectra, which are characterized by very small isotopic shifts that can hardly be detected, using HR CS GFMAS it is feasible to observe several molecular transitions corresponding to $Ca^{79}Br$ and $Ca^{81}Br$ that are spectrally resolved (i.e. they act like two different molecules absorbing at different wavelengths), and can be simultaneously quantified.

The method developed relies on the addition of both Pd and Ca (as chemical modifier and molecule forming agent, respectively), the selection of peak height values and the use of

IBC-m (iterative baseline correction for the monitoring of molecules) for setting the baseline. This method enables accurate Br isotopic analysis in 10 mg L^{-1} solutions with precision values around 2.5% RSD, without requiring any method for mass bias correction.

Moreover, it is also demonstrated how the use of isotope dilution for calibration can help in circumventing severe chemical interferences (e.g., deriving from the presence of high amounts of Cl) when aiming at the direct determination of Br in solid samples by HR CS GFMAS. The accuracy of the method was evaluated *via* analysis of two different reference materials, poly(vinyl chloride) and tomato leaves.

1. Introduction

Br is a halogen found in nature in several matrices such as soil, biomass, peat and coal, but its highest concentration is found in marine waters, lakes, and underground brines associated to oil.[1] It is present in animals as bromide and, recently, it was discovered that it is a cofactor for peroxidasin-catalyzed formation of sulfilimine crosslinks.[2] It is used in drilling fluids, pesticides and brominated flame-retardants.[3] These substances are generally toxic, and may show carcinogenic potential. Therefore, there are several studies that evaluate their presence in the environment, their bioaccumulation in animals,[4,5] and the consequences of human exposure to these compounds.[6,7]

Different analytical techniques have been evaluated to achieve this goal, including for instance Raman spectroscopy,[8] different types of X-ray fluorescence spectrometry (XRF),[8] such as total reflection XRF,[9] wavelength dispersive XRF[10,11] and energy dispersive XRF,[12] neutron activation analysis,[13] inductively coupled plasma optical emission spectrometry (ICP-OES),[12,14] and ion chromatography with different detection techniques (such as UV or conductivity).[15] In addition to these techniques, inductively coupled plasma mass spectrometry (ICP-MS) has been also deployed for Br determination.[16-18] The combination of this technique with different sample introduction systems, such as electrothermal vaporization,[19] capillary electrophoresis,[20] laser ablation,[21] or vapor generation,[22] enhances the potential to determine trace levels of Br in different contexts.

A characteristic of MS is the possibility to offer isotopic information. The importance of isotopic assessment is undeniable. Br isotopic analysis may provide relevant information, for instance, to determine sources of formation waters and hydrogeological processes, or for contamination studies.[23-25] Also, it may help in attaining accurate results by the application of isotope dilution (ID) for calibration.[26-28] Br possesses two stable isotopes (^{79}Br and ^{81}Br) and their natural ratio is close to unity (approximately 1.03 for ^{79}Br/^{81}Br).

Next to the use of MS techniques, the use of optical techniques is being proposed for isotopic analysis in recent literature. One of the reasons is that these techniques may require less extensive sample preparation steps, even if the precision of the results is not as high. In

particular, laser ablation molecular isotopic spectrometry (LAMIS) has been successfully deployed for the isotopic analysis of a number of elements, including boron, carbon, hydrogen, oxygen and strontium.[29-31]

LAMIS was developed by Russo *et al*.[29] and derives from laser induced breakdown spectrometry (LIBS). However, instead of aiming at the monitoring of the emission spectra of elemental species, which show only very small isotopic variations, its purpose is to evaluate and quantify the isotopic shifts occurring for diatomic molecules, in which one of the atoms is the target analyte.

Another technique that has progressed very significantly over the last decade is high-resolution continuum source graphite furnace atomic absorption spectrometry (HR CS GFAAS). This technique offers relevant features such a potential for direct solid sampling,[32] enhanced sensitivity and selectivity (owing to its ability to detect and correct for spectral interferences) and very high spectral resolution (down to 1 pm, depending on the wavelength).[33-37]

Moreover, these features can be deployed not only for monitoring atomic lines, but also for the monitoring of molecular transitions, thus resulting in high-resolution continuum source graphite furnace molecular absorption spectrometry (HR CS GFMAS). HR CS GFMAS not only opens new ways to determine non-metals,[38-40] but also, in a similar way as LAMIS does when compared to LIBS, it may enable attaining isotopic information by investigating the spectrum of diatomic molecules that show an isotopic shift large enough to be monitored and quantified.

The potential of such strategy has been explored only once, in a previous work of our research group devoted to Cl isotopic analysis, selecting AlCl as the target molecule.[41] It is the goal of this work to further investigate whether this approach can be applied to Br as well and, also, for the first time, whether it can be used to improve the quality of results obtained *via* direct solid sampling. Therefore, the aim of this work is the evaluation of the isotopic shift of Br *via* monitoring of the spectrum of the CaBr molecule, and its application to direct solid sampling (SS) in matrices with high content of Cl.

2. Experimental

2.1. Instrumentation

A high-resolution continuum source atomic absorption spectrometer contrAA 700 (Analytik Jena, Germany) equipped with a transversely heated graphite tube atomizer was used throughout this work.[42] The instrument is also equipped with an automated accessory for solid sampling that contains a balance (1 µg precision). Pyrolytic graphite tubes for solid sampling (no dosing hole) were used together with graphite platforms. **Table 1** summarizes the instrumental parameters used during Br determination *via* CaBr monitoring.

2.2 Standards, samples and reagents

Two Br solutions were used for isotopic evaluation: a 1000 mg L^{-1} Br standard solution (Merck, Germany) that shows the natural isotope composition (^{79}Br atom percent: 50.7%; ^{81}Br atom percent: 49.3%), and a 1.00 g L^{-1} Br solution prepared by dissolving a NaBr salt enriched in ^{81}Br (abundance 99.62%, available from CK Gas Products Ltd, UK) in pure water.

A 10 g L^{-1} standard solution Pd (Merck) was diluted to 3 g L^{-1} and used as chemical modifier during optimizations. On the other hand, Pd nanoparticles (PdNP) with a Pd concentration of 500 mg L^{-1} were prepared as described elsewhere.[43] A 10 g L^{-1} Ca solution was prepared by dissolving $CaCO_3$ (Merck) in HNO_3 5% v v^{-1} (Merck) and used as reagent to generate CaBr. A Cl solution of 1000 mg L^{-1} (Merck) was used to investigate the potential interference of this element during analysis. All reagents were of analytical or higher purity.

Lastly, two certified reference materials (CRM) with known Br content and that also show a high Cl content were selected for analysis: a Poly(vinyl chloride) (PVC) sample, PVC-H-07-A Heavy Metals in Poly(vinyl chloride), purchased from Modern Analytical Techniques LLC (USA), and a Standard Reference Material (SRM) available from the National Institute of Standards and Technology (NIST, USA), NIST SRM 1573a Tomato Leaves.

2.3. Analysis of samples

The samples were analyzed directly by HR CS GFMAS following the instrumental parameters shown in **Table 1**. The solid sampling device used enables the automatic

weighing and transport of the samples into the furnace. All these operations are fully controlled by the computer, except for the deposition of the sample, which was carried out manually.

The sample NIST SRM 1573a was already available as a fine powder, requiring no further preparation. The sample PCV-H-07-A is provided as a disc, with a diameter of approximately 31 mm and 13 mm of thickness. Therefore, for this material, aliquots of appropriate mass (see **Table 1**) were cut with a ceramic knife prior to analysis.

Two calibration methods were compared, a calibration curve ranging from 50 to 300 ng of Br, and isotopic dilution with a spike (a 3.11 mmol L^{-1} Br solution) enriched in ^{81}Br (molar isotopic $^{79}Br/^{81}Br$ ratio equal to 0.343). In the case of isotope dilution, the sample was first deposited into the platform and weighed. Later on, the isotopic spike (2.5 µL) plus the solutions containing Ca and PdNPs (10 µL in each case) were deposited on top of the sample using a micropipette. The mixture was then introduced into the furnace and subjected to the temperature program shown in **Table 1**. It was evaluated if it could be preferable to wait up to 2 minutes before starting the temperature program in order to ensure proper mixing, but the results demonstrated that such step was not necessary.

3. Results and discussion

3.1. Br monitoring by HR CS GFMAS

3.1.1. Theoretical and experimental Br isotopic monitoring

As discussed in the introduction, the development of HR CS GFMAS has brought new possibilities to determine non-metals in a graphite furnace. This is typically achieved by monitoring the molecular spectrum of diatomic molecules that show enough thermal stability to resist the relatively high temperatures at which a graphite furnace operates. However, the number of articles devoted to Br determination is still scarce.

Three different molecules have been evaluated so far for this purpose: AlBr,[44] CaBr,[44-47] and SrBr.[48] From the point of view of the stability of the molecule, AlBr offers the highest value (bond dissociation energy: 429 kJ mol^{-1} for AlBr, 339 kJ mol^{-1} for CaBr and 333 kJ mol^{-1} for

SrBr). However, the sensitivity and the isotopic shifts offered by the different molecules need also to be taken into account, considering the aim of the current work.

$$\Delta\nu = (1-\rho)\left[\omega'_e\left(v'+\frac{1}{2}\right)-\omega''_e\left(v''+\frac{1}{2}\right)\right]-(1-\rho^2)\left[\omega'_e x'_e\left(v'+\frac{1}{2}\right)^2-\omega''_e x''_e\left(v''+\frac{1}{2}\right)^2\right] \quad (1)$$

The theoretical isotope shifts were calculated for every molecule (AlBr, CaBr and SrBr, but also BaBr was explored as an alternative) with equation (1), available from ref. 49. In this equation, $\Delta\nu$ is the isotopic shift in cm^{-1}, ν is the vibrational quantum number, ω_e is the harmonic frequency, $\omega_e x_e$ and $\omega_e y_e$ are the first and second anharmonic constants, respectively, and $\rho=(\mu/\mu^i)^{1/2}$, where μ is the reduced mass of the molecule and i corresponds to the heavier isotope. The number of apostrophes denotes the electronic level (two for the lower one, and one for the upper one) involved in the electronic transition.[41] These results, together with experimental data when available, are shown in **Table 2**.

Typically, the most sensitive transitions are those with 0,0 as vibrational numbers, but those offer a very small isotopic shift, according to eq. 1 (the shift increases with the difference between the vibrational levels), and therefore exploring alternative transitions is necessary. For instance, a good agreement between the theoretical and experimentally observed isotopic shift values was found for AlBr electronic transition $X^1\Sigma \rightarrow A^1\Pi$, and such shift (over 22 pm) is large enough for HR CS GFMAS monitoring (see **Figure 1a**). However, the sensitivity of this transition is very low (0.0065 μg^{-1}, using the peak height signal with three pixels) and the baseline was not very stable. The same occurs with BaBr, a shift can be clearly appreciated (see **Figure 1b**) but the sensitivity is also poor (0.035 μg^{-1}). SrBr offered an even lower sensitivity, as the isotopic signals could not be seen for 1 µg Br. Therefore, CaBr was investigated instead. It can be mentioned that Ca is not monoisotopic, but its main isotope (^{40}Ca) shows an abundance close to 97%. This means that in practice the sensitivity of the compounds produced with other isotopes is negligible. All the measurements in this work refer to ^{40}Ca.

CaBr electronic transition most commonly used for HR CS GFMAS is $X^2\Sigma \rightarrow A^2\Pi$,[45-47] because it offers the best sensitivity (at 625.315 nm). However, the theoretical isotopic shift

at 625.315 nm is too small (0.22 pm) for the instrumental resolution available, as in this region every detector pixel covers approx. 2.5 pm. Two alternative vibrational transitions, belonging to the same electronic system, are located at 617.68 and 636.48 nm and show promising theoretical isotopic shifts (45.3 and 47.2 pm, respectively); however, their sensitivity is poor, as no signal was detected even with 1 μg of Br. The same occurred for the transitions expected at 404.07 and 400.53 nm.

The only transition that offers both a suitable isotopic shift (in agreement with the value predicted by eq. 1, as it is shown in **Table 2**) and adequate sensitivity was found around 600.24 nm. **Figure 2** illustrates how at this wavelength it was possible to detect the structured bands of both $Ca^{79}Br$ and $Ca^{81}Br$ molecules. The spectrum of this diatomic molecule is significantly different from that observed for the AlCl molecule used for Cl isotopic analysis in a previous work,[41] which showed only two broad peaks for the two different Cl isotopes. In this case, a much more dense spectrum was obtained, but still most of the peaks are sufficiently resolved.

Figure 2 shows the profiles obtained for three different solutions with different molar Br isotopic ratios. As can be seen, several coupled peaks were monitored that responded properly to the 79/81 Br ratio present in the solutions: their ratio was close to unity for the first solution, and then for the other solutions the signal for ^{81}Br increases reversed proportionally to the signal for ^{79}Br. It should be mentioned that, for the sake of clarity and considering that the attribution of the peaks to $Ca^{79}Br$ and $Ca^{81}Br$ is relatively easy to perform, not all of the peaks were highlighted in the figure.

Of the different line couples that could be used, those found at 600.467 nm ($Ca^{81}Br$) and 600.492 nm ($Ca^{79}Br$) showed good sensitivity, resolution and agreement with the expected ratios, and were selected for further work.

An interesting behavior was observed during this study. The total Br content was always constant. Only the Br isotopic composition changed for the three different solutions measured. While for most peaks the signals increased or decreased depending on the 79/81 Br ratio added, as expected, two of them (600.323 and 600.422 nm, labeled with Br in

Figure 2) showed a constant absorbance value. Therefore, these two wavelengths could be used for the determination of elemental Br, with no isotopic profile. They show good linearity at least up to 2500 ng.

3.1.2. Optimization of the working parameters

Obviously, the amount of Ca added should be optimized, because it is necessary to add sufficient Ca to ensure that practically all Br present will produce CaBr molecules. Use of a chemical modifier should also be tested, because it may play an important role during the pyrolysis, helping to prevent the losses of volatile Br species. Pd, added as $Pd(NO_3)_2$ solution, was evaluated for that purpose.

As shown in **Figure 3a,** the CaBr absorbance (monitored at the wavelength of 600.422 nm, which is one of the elemental peaks, thus offering more sensitivity) increases until an amount of 100 µg Ca is reached. Use of higher amounts of Ca resulted in a signal decrease. In any case, this is already a very high value for a GFAAS device and using more is detrimental for the lifetime of the tubes and platforms. Therefore, the Ca mass was set to 100 µg.

In the case of Pd, the absorbance stabilizes around 5 µg (**Figure 3b**). A mass of 10 µg Pd was applied throughout method development to ensure the best performance.

Finally, the temperature program was optimized and the results are shown in **Figure 4**. The behavior found was in good agreement with the literature.[45-47] It is however important to confirm that the ratio of the $Ca^{79}Br$ and $Ca^{81}Br$ absorbance signals remained practically constant with the temperature. A pyrolysis of 700 ºC was sufficient to attain well-defined signal profiles and was thus selected. As for the vaporization, a value of 2200 ºC seems to provide the maximum sensitivity, so it was chosen for further work.

3.2. Isotopic shift signal evaluation

Peak height was used for CaBr signal quantification instead of peak area, as it showed the best agreement with the expected ratios. This probably occurs because the influence of the structured background becomes higher when using peak areas.[41] Subsequently, two other

factors related with signal evaluation were studied in detail: the number of detector pixels selected and, particularly, the procedure used to set the baseline.

The last software version of the spectrometer provides a number of ways to set the baseline. In the past, it was only possible to choose between a dynamic mode (where the software establishes the baseline automatically), or a static mode, where the operator manually selects the pixels used to set the baseline (e.g., by choosing the valleys between the main peaks). While the dynamic mode works very accurately for atomic spectra, where only a few lines are monitored, it is clearly not appropriate for a dense molecular spectrum with many lines, as discussed elsewhere.[40,50]

Recently, two more modes based on a new baseline correction algorithm have been made available. These are named IBC (iterative baseline correction) and IBC-m, respectively, the latter being supposed to be more suitable for the monitoring of molecules. The exact details of how these algorithms work are not disclosed, but their application helps in reducing the width of the lines at the cost of lowering a bit their maximum value. This fact suggests the use of some moving average. This effect helps in establishing the baseline more correctly and, also, minimizes signal overlaps.

Setting the baseline properly may be critical for accurate isotopic analysis, and thus three different modes (static, IBC and IBC-m) were compared to evaluate which one was more suitable in the context of this work.

Therefore, five Br (as NaBr) solutions with different $^{79}Br/^{81}Br$ isotopic ratios, ranging from 0.117 to 0.685, were prepared. Five spectra were obtained for each solution and the three different baseline modes were applied to them. Moreover, the number of detector pixels was also evaluated, comparing the use of just the central pixel (CP), the three central pixels (CP±1), or the five central pixels (CP ± 2), for each peak. The pixels 60, 72, 106, 126, and 142 were selected for the static mode to set the baseline. All the measurements were centered at 600.422 nm, and the signals located at 600.467 ($Ca^{81}Br$) and 600.492 nm ($Ca^{79}Br$) were used for quantification.

Figure 5 shows the results obtained when plotting the theoretical and experimental $^{79}Br/^{81}Br$ ratios. As can be seen, a good agreement was found in most cases, with a squared correlation coefficient (R^2) higher than 0.967. However, the best agreement with the expected values was found for IBC-m ($R^2 \geq 0.991$), followed by IBC ($R^2 \geq 0.987$) and, finally, by the static mode ($R^2 \geq 0.967$), the latter being clearly not suitable as the deviation from the expected values were high (up to 15-20%) for some points. Thus, IBC-m was chosen for further work.

As for the number of detector pixels selected, the difference between using three and five pixels was very small. However, for the highest difference in abundance (ratio 0.117) the results tend to be biased low if five pixels are used. This probably occurs because the low $Ca^{79}Br$ signal is affected by the background noise when less sensitive side pixels are added. Therefore, the three central pixels were selected. Other pair of isotopic peaks present in this region was also evaluated (600.359 nm $Ca^{81}Br$, and 600.389 nm $Ca^{79}Br$), and its behavior showed no significant difference with that discussed above.

Once the optimum conditions were established, 20 replicate measurements of a Br solution of known (natural) isotopic composition were carried out. The results are shown in **Figure 6**. As can be seen, the typical variation observed for every individual isotopic CaBr transition is rather high (approx. 6%), but when isotope ratios are calculated a much better value is obtained, as all the correlated sources of noise are compensated. In this way, a 2.6 % RSD value can be considered as typical for Br isotopic analysis under these conditions.

This value is clearly insufficient if the goal is to monitor natural Br isotopic variations. However, it may be enough for performing tracer experiments or for using isotope dilution for calibration, as will be demonstrated in section 3.4. Furthermore, it can be stressed that, with this technique, an accurate ratio, within the uncertainty indicated above, is directly obtained without the need for any type of mass bias correction, unlike what occurs with most MS techniques.

3.3. Cl Interference in the monitoring of CaBr

One of the disadvantages of using GFMAS instead of GFAAS is that the probability to suffer from chemical interferences increases significantly because, depending on the matrix composition, the formation of molecules different from the targeted one may be favored.

For instance, Br determination is susceptible to suffer interferences from Cl, because Cl generally binds more strongly with metals than Br. The elimination of Cl during sample preparation, without Br losses, is not trivial, due to their chemical similarity. Moreover, the concentration of Cl in nature is approximately 650 times higher than that of Br,[51] a factor that cannot be neglected. As a result, in many samples there would be a competition between both halogens to react with Ca. In this circumstance, CaCl (CaCl: 409 kJ mol^{-1}) would be generated more efficiently than CaBr (339 kJ mol^{-1}).[52]

Therefore, a study was carried out to evaluate the effect of the presence of Cl on the formation of CaBr. **Figure 7a** shows the results. It is clear that Cl may interfere severely in the formation of CaBr. When the Cl molar content equals the Br molar content, the CaBr signal decreases by more than 20%. When the number of Cl moles is approximately ten times the number of Br moles, the remaining CaBr absorbance is only 20% of the initial signal. This is obviously a significant problem for the determination of Br as CaBr. Not only it will result in a loss of sensitivity, but, moreover, it will be difficult to develop a simple calibration strategy for a sample of unknown Cl content.

Despite the influence exerted by Cl, **Figure 7b** shows that there is almost no fluctuation in the $Ca^{79}Br/Ca^{81}Br$ absorbance ratio obtained for different Cl amounts. The only exception is the last point, because the absorbance of the $Ca^{79}Br$ and $Ca^{81}Br$ molecules is already too low to obtain a reproducible ratio. This fact indicates that, as long as it is possible to obtain a sufficiently high signal, the use of isotope dilution for calibration may properly correct for this chemical interference.

3.4. Determination of Br in solid samples by isotope dilution

The method was further optimized aiming at the direct determination of Br in solid samples. Two different materials showing a high Cl content (6600 mg kg^{-1} for SRM 1573a, and approx. 55% for PVC) were selected as a proof of concept.

The main goal was to check if the use of ID for calibration could help in circumventing the interferences expected when trying to analyze these samples by means of SS HR CS GFMAS. Moreover, these applications are of practical interest. Determination of Br in plastics is needed due to the use of Br-based flame retardants, which are persistent pollutants.[7,8,17,47] Also, the toxicity of many Br compounds makes its determination required in biological samples, including plants.[1,3]

The optimum conditions for solid sampling are not always equivalent to those established for measuring solutions. Investigating a number of aspects such as a) different pyrolysis and vaporization temperatures; b) different chemical modifiers; c) the effect of the sample mass; and, d) the wavelength more suitable for the sample content, is generally required.[32] Therefore, all these topics were studied.

The addition of 10 µg Pd (as $Pd(NO_3)_2$) did not seem to be sufficient to stabilize Br in the graphite furnace at the pyrolysis temperatures necessary for efficient matrix removal (400 ºC for tomato leaves, 1000 ºC for PVC). The use of higher amounts of Pd did not help either. As an alternative, the use of Pd nanoparticles (NPs) was tested.

PdNPs already provided a superior performance in comparison with other Pd forms when aiming at the determination of another non-metal known to form volatile species (sulfur) in different solid samples[43] and in diesel fuel,[53] respectively. The reasons for the higher efficiency of the PdNPs are discussed elsewhere[43] and will not be repeated. A PdNP suspension was prepared as described in ref. 43 and it was found that the addition of 5 µg of PdNPs permitted to obtain well-defined CaBr signals for the solid samples by HR CS GFMAS. The optimum amount of Ca was evaluated, but maximum signals were again found for 100 µg.

The temperature program was also optimized, aiming at maximum sensitivity, and the values finally chosen are listed in **Table 1**. As could be anticipated, it is necessary to use a higher temperature to properly vaporize Br and form the CaBr molecule when a solid sample is directly analyzed (2400 ºC instead of 2200 ºC for solutions).

After these optimizations, a calibration curve with Br standard solutions (ranging from 50 to 300 ng Br) was prepared and direct analysis of the samples by means of SS HR CS GFMAS was attempted, using CaBr most sensitive transition (625.315 nm). The figures of merit for this calibration were R^2=0.9991 and a limit of detection (LOD) of 4.0 ng. The results obtained are shown in **Table 3**.

As can be seen, the results obtained for both samples are biased low very significantly. It appears that, despite all the efforts for optimization, the amount of Br that finally produces CaBr is very low for these solid samples. This is most likely owing to the Cl competition, as discussed in the previous section, and therefore a simple calibration approach with aqueous standards cannot provide accurate results. However, use of ID could circumvent this problem, providing a proper equilibration of the Br present in the solid sample and in the spike (added as liquid) is achieved during the progress of the temperature program.

That implies that, at some point during the development of the temperature program (either after the drying and the pyrolysis steps, in solid phase or, more likely, later on, in gas phase), the Br species originating from the solid sample and from the spike should mix properly and evolve to a similar chemical state. In this way, both should be equally affected by the interference (Cl) and, therefore, the ratio finally obtained would reflect the correct composition of the mixture. This approach was thus investigated.

As shown in **Figure 8**, well defined and unimodal CaBr absorption peaks were obtained when monitoring the mixtures of the spike and the solid samples. This fact indicates that the above-mentioned Br equilibration may have been achieved under the conditions applied. Furthermore, a result in good agreement with the reference value was attained with ID SS HR CS GFMAS, as indicated in **Table 3**. The use of ID in combination with direct solid sampling HR CS GFMAS was not reported before, and provides a powerful tool to overcome the chemical interferences that sometimes hamper the use of this technique.

As for the imprecision, the values obtained (4-8 %RSD) can be considered as typical for the technique and should be mainly attributed to the sample inhomogeneity, which is of course not corrected for when using ID. Therefore, an appropriate sample mass (not exceeding a

few milligrams owing to size limitations) and a proper number of replicates should be selected to obtain a representative result.[32]

One of the disadvantages of this approach is the loss of sensitivity because, as discussed in section 3.1., those transitions that show a clear isotopic shift are typically less sensitive than the main head bands (in this case, a factor of 10). However, this sacrifice can be justified considering that such a severe chemical interference can be resolved. The limit of quantification obtained for the ID approach was estimated to be 60 ng (which means approx. 3 mg L^{-1} for solutions, using a volume of 20 µL, or 30 µg g^{-1} for solid samples, using a sample mass of 2 mg), as for lower values it was difficult to achieve a reproducible $^{79}Br/^{81}Br$ ratio.

4. Conclusion

The potential of HR CS GFMAS for the isotopic analysis of Br was demonstrated for the first time. The results confirm that, by monitoring molecular instead of atomic spectra, in the presence of Ca, it is possible to appreciate different pairs of $Ca^{79}Br$ and $Ca^{81}Br$ transitions that are sufficiently well resolved spectrally (approx. 42 pm) to enable their selective quantification and the subsequent calculation of the 79/81 Br ratio found in the sample. Furthermore, there are also other lines that appear simultaneously and provide elemental information corresponding to Br (probably an overlap of $Ca^{79}Br$ and $Ca^{81}Br$ peaks), which can be used for optimization due to their higher sensitivity.

The method developed is based on the addition of Pd and Ca, the monitoring of peak height values, and the use of IBC-m mode for setting the baseline. Such method enables the isotopic analysis of Br at the mg L^{-1} level with precision values around 2.5 % RSD, not requiring any method for mass bias correction.

Finally, it was corroborated that using ID for calibration is possible in this context, and provides a novel and a very powerful strategy to determine Br in complex samples. In fact, it was demonstrated that using ID it is feasible to carry out the direct determination of Br in solid samples in the presence of high amounts of interfering Cl, even if the spike is added as

solution. This approach opens new possibilities for the direct analysis of solid samples by HR CS GFMAS.

5. Acknowledgments

This work has been funded by the Spanish Ministry of Economy and Competitiveness (project CTQ2015-64684-P) and the Aragón Government (Fondo Social Europeo and project Innova-A1-020-15). The authors are also grateful to Fundação de Amparo à Pesquisa do Estado de São Paulo (FAPESP) for the financial support (grant#2014/24430-7).

References

1. P. Vainikka and M. Hupa, *Fuel*, 2012, **95**, 1–14.

2. A.S. McCall, C.F. Cummings, G. Bhave, R. Vanacore, A. Page-McCaw and B.G. Hudson, *Cell*, 2014, **157**, 1380–1392.

3. P. Vainikka and M. Hupa, *Fuel*, 2012, **94**, 34–51.

4. N. Cappelletti, E. Speranza, L. Tatone, M. Astoviza, M.C. Migoya and J.C. Colombo, *Environ. Sci. Pollut. Res.*, 2015, **22**, 7093–7100.

5. D. Chen and R.C. Hale, *Environ. Int.*, 2010, **35**, 800–811.

6. K. Ni, Y. Lu, T. Wang, K. Kannan, J. Gosens, L. Xu, Q. Li, L. Wang and S. Liu, *Int. J. Hyg. Environ. Health*, 2013, **2016**, 607–623.

7. V. Linares, M. Bellés and J.L. Domingo, *Arch. Toxicol.*, 2015, **89**, 335–356.

8. R. Taurino, M. Cannio, T. Mafredini and P. Pozzi, *Environ. Technol.*, 2014, **35**, 3147–3152.

9. H. Fink, U. Panne, M. Theisen, R. Niessner, T. Probst and X. Lin, *Fresenius J. Anal. Chem.*, 2000, **368**, 235–239.

10. T. Gorewoda, Z. Mzyk, J. Anyszkiewicz and J. Charasińska, *Spectrochim. Acta Part B*, 2015, **106**, 8–12.

11. J. An, H. Jung, J.-R. Bae, H.-O. Yoon and J. Seo, *Spectrochim. Acta Part B*, 2014, **91**, 1–4.

12. N. Miskolczi, W.J. Hall, N. Borsodi, P.T. Williams and A. Angyal, *Microchem. J.*, 2011, **99**, 60–66.

13. T. Miura, R. Okumura, Y. Iinuma, S. Sekimoto, K. Takamiya, M. Ohata and A. Hioki, *J. Radioanal. Nucl. Chem*, 2015, **303**, 1417–1420.

14. J. Naozuka, M.A.M.S. da Veiga, P.V. Oliveira and E. de Oliveira, *J. Anal. At. Spectrom.*, 2003, **18**, 917–921.

15. B. López-Ruiz, *J. Chromatogr. A*, 2000, **881**, 607–627.

16. R.S. Picoloto, S.M. Cruz, P.A. Mello, E.I. Muller, P. Smichowski and E.M.M. Flores, *Microchem. J.*, 2014, **116**, 225–229.

17. A. Solá Vázquez, J.M. Costa-Fernández, J. Ruiz Encinar, R. Pereiro and A. Sanz-Medel, *Anal. Chim. Acta*, 2008, **623**, 140–145.

18. A.L.H. Muller, P.A. Mello, M.F. Mesko, F.A. Duarte, V.L. Dressler, E.I. Muller and E.M.M. Flores, *J. Anal. At. Spectrom.*, 2012, **27**, 1889–1894.

19. J.S. de Gois, É.R. Pereira, B. Welz and D.L.G. Borges, *Anal. Chim. Acta*, 2014, **852**, 82–87.

20. J.-H. Chen, K.-en Wang and S.-J. Jiang, *Electrophoresis*, 2007, **28**, 4227–4232.

21. B. Izgi and M. Kayar, *Talanta*, 2015, **139**, 117–122.

22. R.E. Sturgeon, *Anal. Chem.*, 2015, **87**, 3072–3079.

23. F. Gelman and L. Halicz, *Int. J. Mass Spectrom.*, 2010, **289**, 167–169.

24. O. Shouakar-Stash, S.K. Frape and R.J. Drimmie, *Anal. Chem.*, 2005, **77**, 4027–4033.

25. J.S. de Gois, P. Vallelonga, A. Spolaor, V. Devulder, D.L.G. Borges and F. Vanhaecke, *Anal. Bioanal. Chem.,* 2016, **408**, 409–416.

26. A. González-Gago, J.M. Marchante-Gayón, M. Ferrero and J.I.G. Alonso, *Anal. Chem.*, 2010, **82**, 2879–2887.

27. F. Cuyckens, L.I.L. Balcaen, K. De Wolf, B. De Samber, C. Van Looveren, R. Hurkmans and F. Vanhaecke, *Anal. Bioanal. Chem.*, 2008, **390**, 1717–1729.

28. M. Ohata and T. Miura, *Anal. Chim. Acta*, 2014, **837**, 23–30.

29. R.E. Russo, A.A. Bol'shakov, X. Mao, C.P. McKay, D.L. Perry and O. Sorkhabi, *Spectrochim. Acta Part B,* 2011, **66**, 99–104.

30. R.E. Russo, X. Mao, J.J. Gonzalez, V. Zorba and J. Yoo, *Anal. Chem.*, 2013, **85**, 6162–

6177.

31. A.A. Bol'shakov, X. Mao, J.J. González and R.E. Russo, *J. Anal. At. Spectrom.*, 2016, **31**, 119–134.

32. M. Resano, M. Aramendía and M.A. Belarra, *J. Anal. At. Spectrom.,* 2014, **29**, 2229–2250.

33. M. Resano, F. Vanhaecke and M.T.C. de Loos-Vollebregt, *J. Anal. At. Spectrom.*, 2008, **23**, 1450-1475.

34. B. Welz, S. Morés, E. Carasek, M.G.R. Vale, M. Okruss and H. Becker-Ross, *Appl. Spectrosc. Rev.*, 2010, **45**, 327–354.

35. M. Resano and E. García-Ruiz, *Anal. Bioanal. Chem.,* 2011, **399**, 323–330.

36. M. Resano, M.R. Flórez and E. García-Ruiz, *Spectrochim. Acta Part B,* 2013, **88**, 85–97.

37. B. Welz, M.G.R. Vale, É.R. Pereira, I.N.B. Castilho and M.B. Dessuy, *J. Braz. Chem. Soc.*, 2014, **25**, 799–821.

38. B. Welz, F.G. Lepri, R.G.O. Araujo, S.L.C. Ferreira, M.D. Huang, M. Okruss and H. Becker-Ross, *Anal. Chim. Acta,* 2009, **647**, 137–148.

39. D.J. Butcher, *Anal. Chim. Acta*, 2013, **804**, 1–15.

40. M. Resano, M.R. Flórez and E. García-Ruiz, *Anal. Bioanal. Chem.*, 2014, **406**, 2239–2259.

41. F.V. Nakadi, M.A.M.S. da Veiga, M. Aramendía, E. García-Ruiz and M. Resano, *J. Anal. At. Spectrom.*, 2015, **30**,1531–1540.

42. B. Welz, H. Becker-Ross, S. Florek and U. Heitmann, *High-Resolution Continuum Source AAS. The Better Way to do Atomic Absorption Spectrometry*, Wiley-VCH, Weinheim, 2005.

43. M. Resano and M. R. Flórez, *J. Anal. At. Spectrom.*, 2012, **27**, 401–412.

44. M.D. Huang, H. Becker-Ross, S. Florek, U. Heitmann and M. Okruss, *Spectrochim. Acta Part B*, 2008, **63**, 566–570.

45. É.R. Pereira, I.N.B. Castilho, B. Welz, J.S. Gois, D.L.G. Borges, E. Carasek and J.B. de Andrade, *Spectrochim. Acta Part B*, 2014, **96**, 33–39.

46. T. Limburg and J.W. Einax, *Microchem. J.*, 2013, **107**, 31–36.

47. M.R. Flórez and M. Resano, *Spectrochim. Acta Part B*, 2013, **88**, 32–39.

48. S. Gunduz and S. Akman, *Microchem. J.*, 2014, **116**, 1–6.

49. G. Herzberg, *Molecular Spectra and Molecule Structure. I. Spectra of Diatomic Molecules*, D. Van Nostrand, 2nd edn, New York, 1950.

50. Z. Kowalewska, *Spectrochim. Acta Part B*, 2011, **66**, 546–556.

51. H.E. Suess and H. C. Urey, *Rev. Mod. Phys.*, 1956, **28**, 53–74.

52. D.R. Lide, *CRC Handbook of Chemistry and Physics*, 90th edn, CRC Press: Boca Ratón, 2009.

53. F.V. Nakadi, A.L.C. Soares and M.A.M.S. da Veiga, *J. Anal. At. Spectrom.*, 2014, **29**, 1871–1879.

54. R.W.B. Pearse and A.G. Gaydon, *The Identification of Molecular Spectra*, Chapman & Hall, 3rd edn, London, 1963.

Table 1. Instrumental parameters used to determine Br as CaBr by HR CS GFMAS. The conditions used for direct analysis of the solid samples (PVC and tomato leaves, see section 3.4.) are indicated by (a) and (b), respectively.

Electronic transition	$X^2\Sigma \rightarrow B^2\Sigma$
Wavelengths	600.467 nm ($Ca^{81}Br$)
	600.492 nm ($Ca^{79}Br$)
Number of detector pixels summed per line	3 (6.40 pm)
Molecule forming agent	Ca (100 µg)
Chemical modifier	Pd (5 µg) nanoparticles
Sample mass	0.5 – 1.8 mg (PVC)
	0.7 – 0.9 mg (tomato leaves)

Temperature program

Step	*Temperature / °C*	*Ramp / °C s^{-1}*	*Hold / s*	*Ar gas flow / L min^{-1}*
Drying	90	3, 5[a,b]	20, 30[a,b]	2.0
Drying	120	5	10, 20[a,b]	2.0
Pyrolysis	700, 1000[a] 400[b]	300, 50[a,b]	25, 55[a,b]	2.0
Vaporization	2200, 2400[a,b]	3000	6	0
Cleaning	2500, 2650[a,b]	500, 1000[a,b]	5	2.0

Table 2 Theoretical ($\Delta\lambda_{calc}$, calculated using eq. 1), and experimental ($\Delta\lambda_{exp}$, as observed using HR CS GFMAS) isotopic shifts for AlBr, BaBr and CaBr band heads. The terms ν' and ν'' represent the vibrational quantum number of the excited and fundamental state, respectively, and n.d. stands for not detected.

λ^a / nm	λ_{exp} / nm	ν', ν''	$\Delta\lambda_{calc}$ / pm	$\Delta\lambda_{exp}$ / pm
AlBr molecule				
Electronic transition $X^1\Sigma \rightarrow A^1\Pi$				
285.53	285.552	1, 3	22.6	22.4
BaBr molecule				
Electronic transition $X^2\Sigma \rightarrow C^2\Pi$				
526.06	526.059	0, 1	43.0	43.3
-	524.749	-	-	27.0
CaBr molecule				
Electronic transition $X^2\Sigma \rightarrow A^2\Pi$				
636.48	n.d.	0, 1	47.2	n.d.
625.29	625.315	0, 0	0.22	n.d.
617.68	n.d.	1, 0	45.3	n.d.
Electronic transition $X^2\Sigma \rightarrow B^2\Sigma$				
610.47	n.d.	0, 0	0.06	n.d.
600.24	600.234	1, 0	42.0	41.6
Electronic transition $X^2\Sigma \rightarrow C^2\Pi$				
404.07	n.d.	0, 2	38.7	n.d.
400.53	n.d.	0, 2	38.0	n.d.

[a]Data on these transitions was obtained from reference 54.

Table 3. Br determination by SS HR CS GFMAS, either constructing the calibration curve with aqueous standard solutions or using isotope dilution for calibration. The experimental uncertainties are expressed as 95% confidence interval (n = 5).

Sample	Br concentration / μg g^{-1}		
	Reference value	SS HR CS GFMAS	ID SS HR CS GFMAS
PVC-H-07-A	1100 ± 44	67 ± 12	1081 ± 112
NIST SRM 1573a Tomato Leaves	1300	102 ± 11	1381 ± 71

Figure captions

Figure 1. (A) AlBr spectrum (maximum peak height) corresponding to the electronic transition $X^1\Sigma \rightarrow A^1\Sigma$ around 285.552 nm obtained by HR CS GFMAS using 10 µg of Br, and 10 µg Al. (B) BaBr spectrum corresponding to electronic transition $X^2\Sigma \rightarrow C^2\Sigma$ around 524.749 nm obtained by HR CS GFMAS using 1 µg of Br, and 10 µg Ba. In both cases, 10 µg of Pd were added as chemical modifier.

Figure 2. CaBr spectra (maximum peak height) observed around 600.24 nm (electronic transition $X^2\Sigma \rightarrow B^2\Sigma$) for three solutions with a different $^{79}Br/^{81}Br$ isotopic ratio content: (—) 1.028, (—) 0.343, and (—) 0.004. These signals were obtained for 0.20 µg of Br, 100 µg Ca, and 10 µg Pd. The labels 79 and 81 highlight the peaks that correspond with the $Ca^{79}Br$ and $Ca^{81}Br$ absorption, respectively, and the label Br marks the elemental lines.

Figure 3. Optimization of the (A) Ca and (B) Pd amount added to monitor CaBr at 600.422 nm by HR CS GFMAS. Both studies were carried out with 0.10 µg total Br, wherein for (A) 10 µg of Pd were always added, and for (B) 100 µg of Ca were chosen. Three central pixels were summed at the maximum peak height for quantification. Error bars represent the standard deviation (n = 5).

Figure 4. Optimization of the pyrolysis and vaporization temperatures for Br monitoring as CaBr by HR CS GFMAS with 0.2 µg of Br (molar ratio $^{79}Br/^{81}Br$: 1.03), at wavelengths 600.467 ($Ca^{81}Br$) and 600.492 nm ($Ca^{79}Br$), with the addition of 100 µg Ca and 10 µg Pd. The pyrolysis temperature was set at 1000 °C for the vaporization study, while 2200 °C was used as vaporization temperature during the pyrolysis study. The three central pixels of each transition were summed at the maximum peak height. Error bars represent standard deviation (n = 5).

Figure 5. Correlation between the experimental (as obtained *via* HR CS GFMAS) and theoretical (as prepared by properly mixing two standards of known ratio and concentration) $^{79}Br/^{81}Br$ molar ratio when monitoring the 600.492 nm ($Ca^{79}Br$) and 600.467 nm ($Ca^{81}Br$) transitions for solutions containing 200 ng of Br, when using: A) IBC-m; B) IBC; and C) the

static modes for setting the baseline, and a different number of detector pixels ((■) CP, (●) CP ± 1, and (▲) CP ± 2). Error bars represent the standard deviation (n=5).

Figure 6. Comparison of the variations observed for a series of 20 replicates for 0.2 µg Br ($^{79}Br/^{81}Br$: 1.03) with 100 µg Ca and 10 µg Pd, when monitoring the individual 600.467 ($Ca^{81}Br$) and 600.492 nm ($Ca^{79}Br$) transitions (left y-axis) or when calculating the Br ratio from the same data set (right y-axis). The blue line represents the average value of the 20 replicates, and the red line represents the natural Br isotopic ratio.

Figure 7. Study of the Cl interference when monitoring the (A) CaBr absorbance at 600.422 nm, and the (B) $Ca^{79}Br/Ca^{81}Br$ absorbance ratio (600.492 and 600.467 nm, respectively), as a function of the Cl content. All the measurements were carried with 0.5 µg Br, 100 µg Ca and 10 µg Pd. The red line represents the Br natural isotopic ratio. Uncertainties are expressed as standard deviation (n = 5).

Figure 8. CaBr three-dimensional spectrum at the region of 600.4 nm obtained by SS HR CS GFMAS upon monitoring of SRM NIST 1573a (approximately 1.0 µg Br) mixed with the spike enriched in ^{81}Br, using the conditions displayed in **Table 1**. The highlighted band heads are the main ones used during all the study: $Ca^{79}Br$ (600.492 nm), $Ca^{81}Br$ (600.467 nm), and CaBr (600.422 nm).

Figure 1

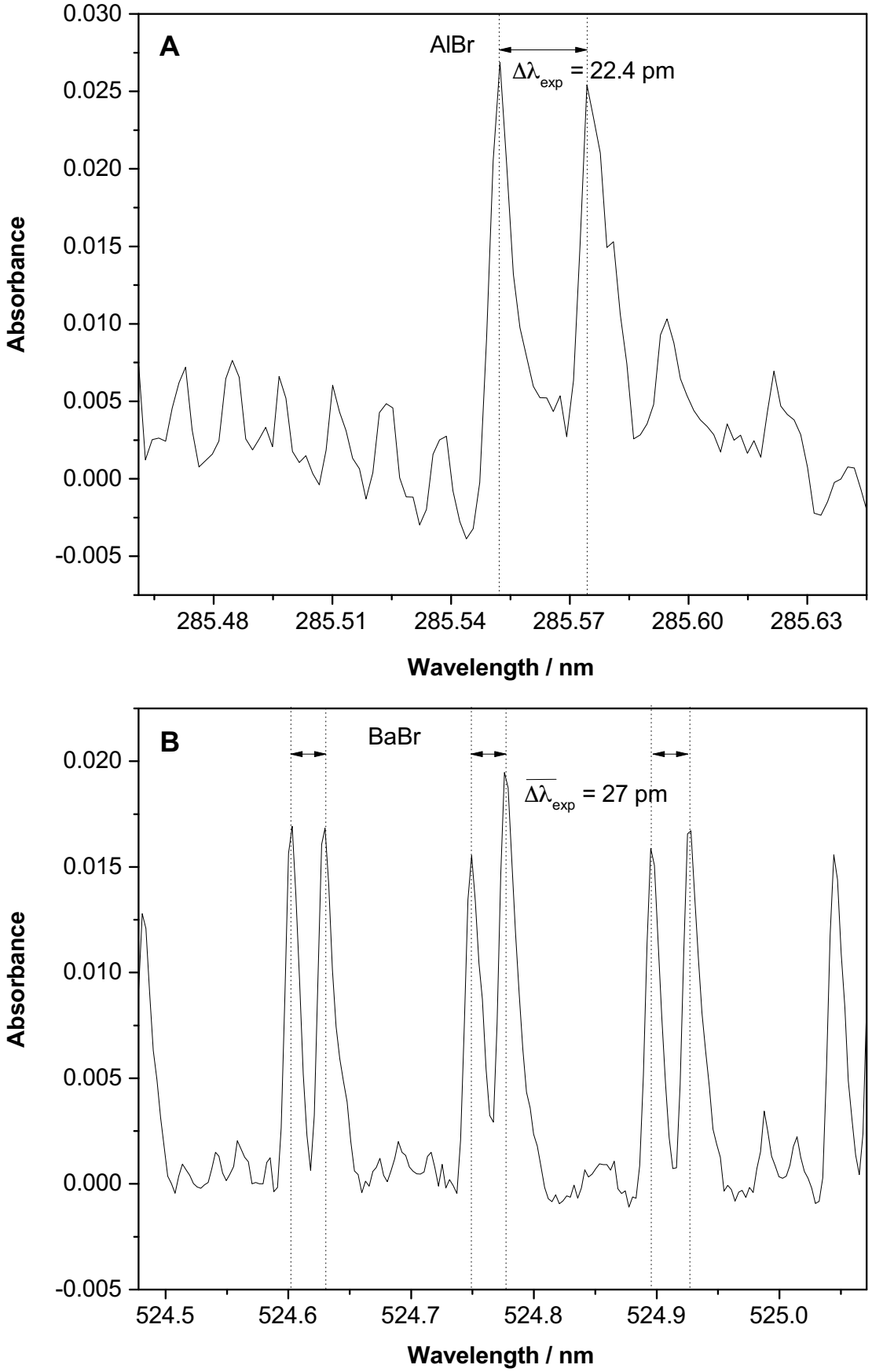

Figure 2

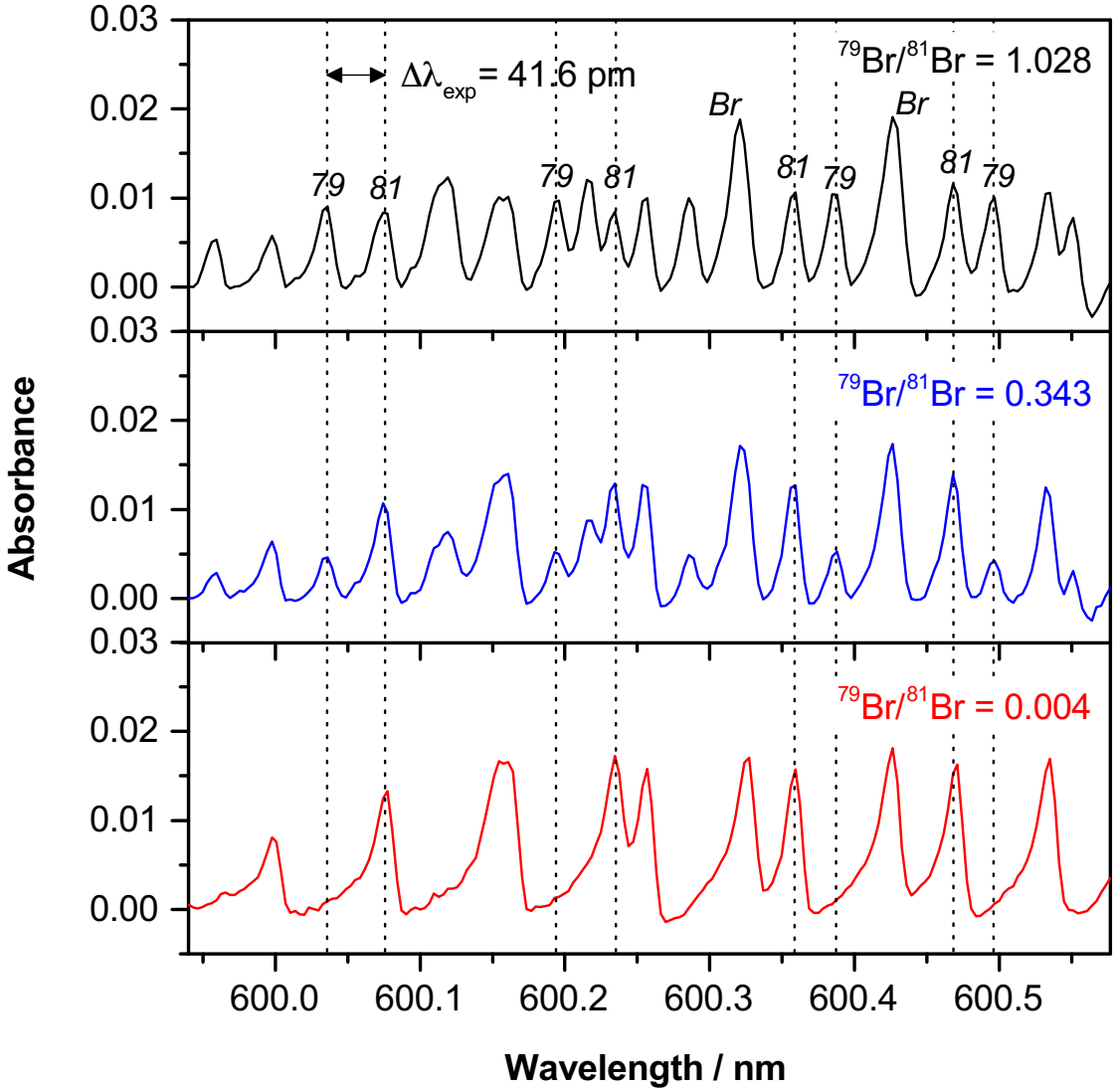

Figure 3

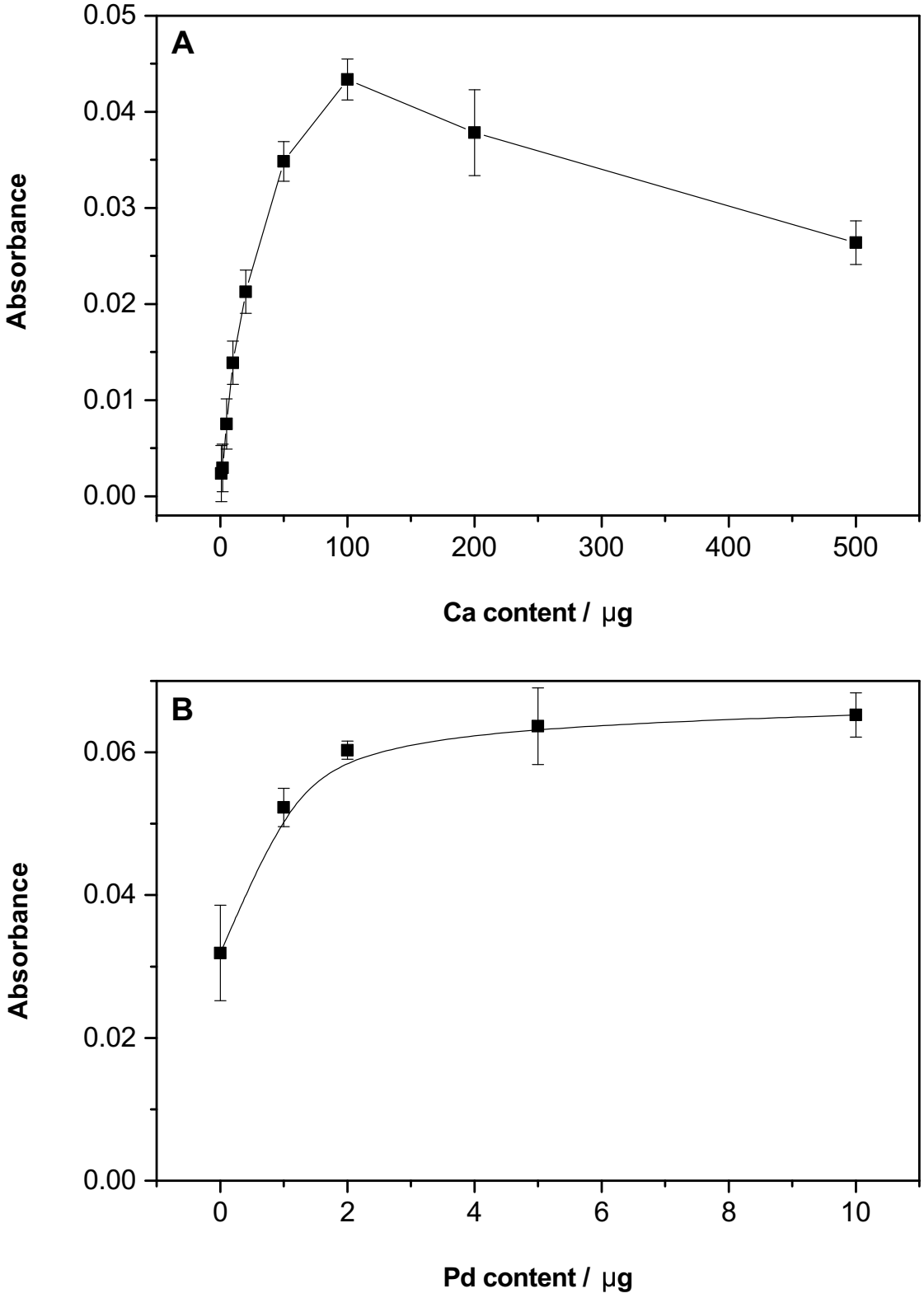

Figure 4

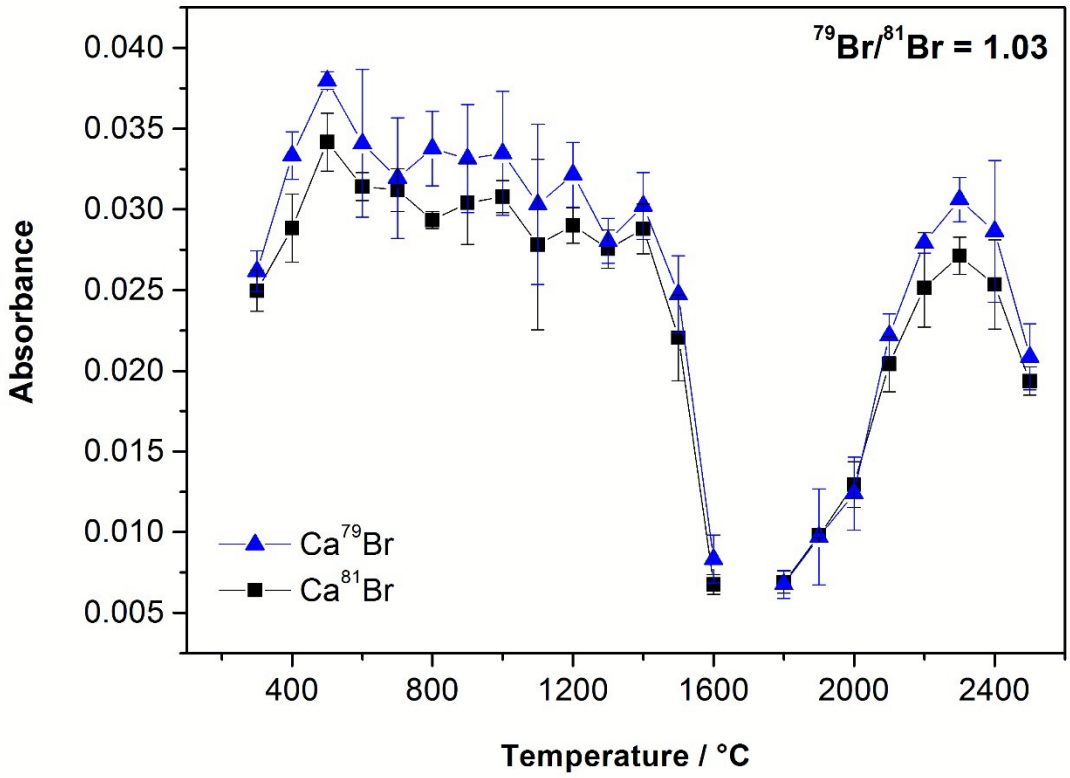

Figure 5

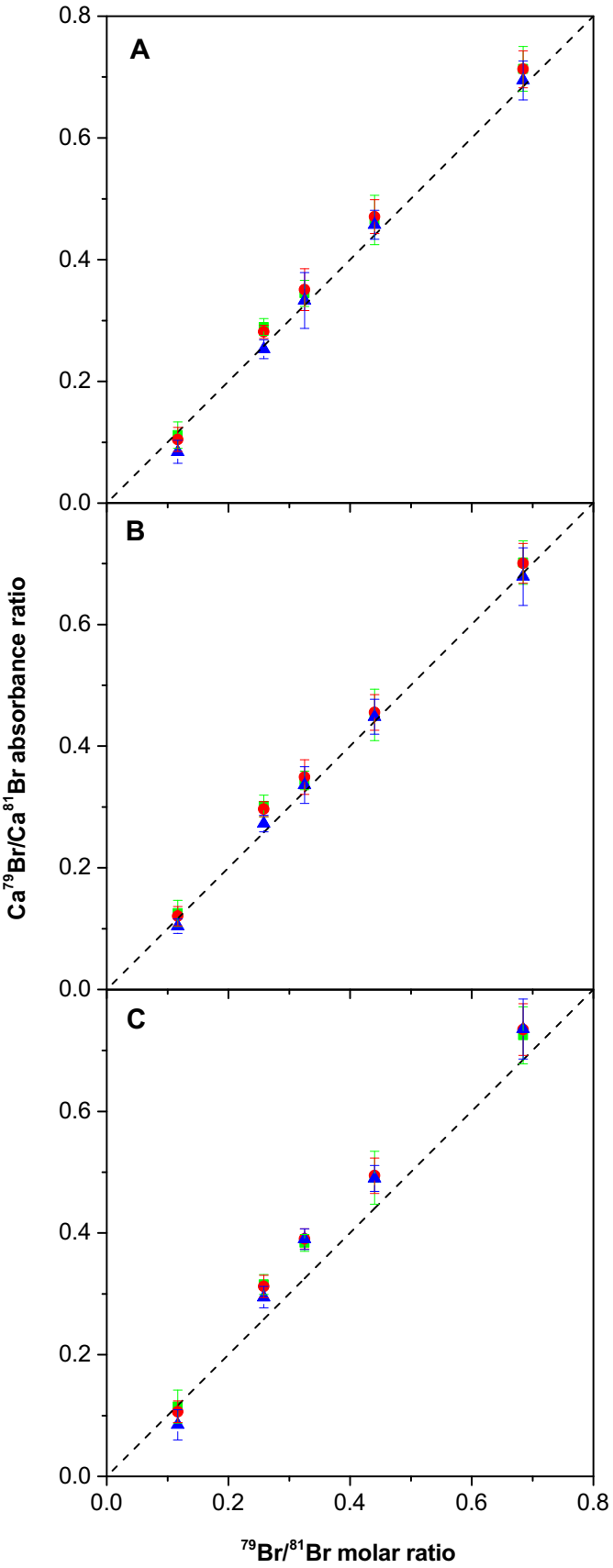

Figure 6

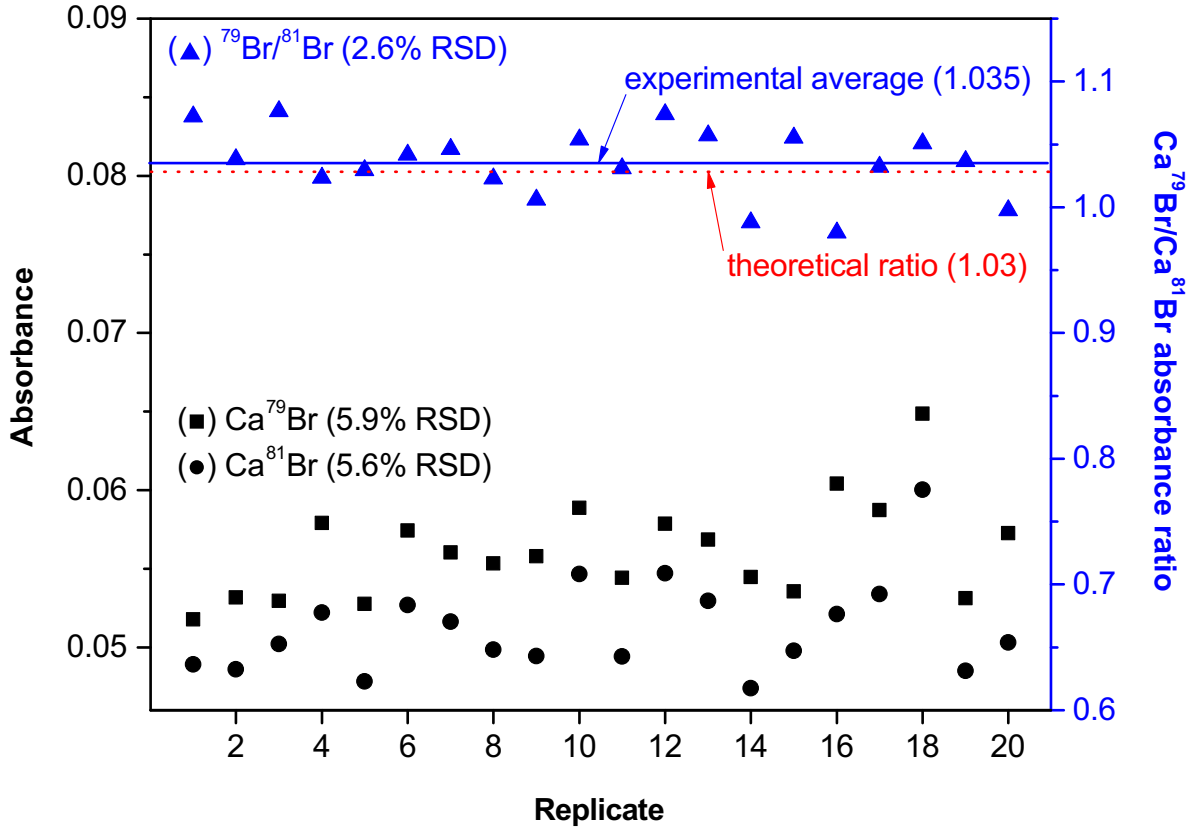

Figure 7

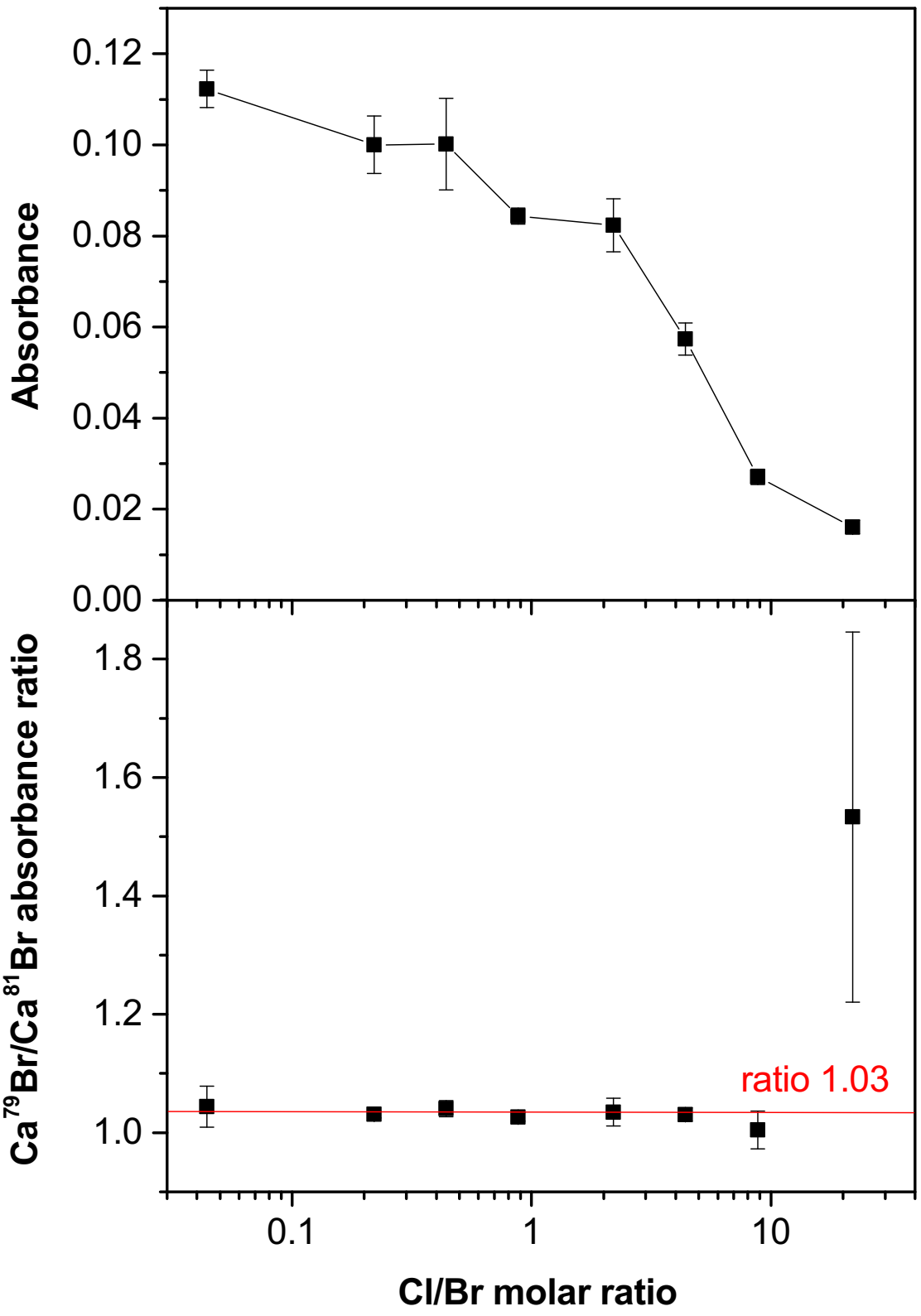

Figure 8